

Simulation of H&V Shield Behavior at Sharp Curve by Kinematic Shield Model

T. N. Huynh¹, H.V. Pham², M. Sugimoto³, Y. Tanaka⁴, H. Ohta⁵ and K. Yasui⁶

^{1,2}Graduate School of Nagaoka University of Technology, Nagaoka, Japan

³Department of Civil and Environmental Engineering, Nagaoka University of Technology, Nagaoka, Japan

^{4,5,6}Tachiaigawa Shield Tunneling Site Office, Shimizu Co. Ltd., Japan

³E-mail: sugimo@vos.nagaokaut.ac.jp

ABSTRACT: Due to the restrictions of underground space use, the horizontal and vertical variation shield method (H&V shield) was innovated, of which the cross section is changed from horizontal multi-circular shape to vertical one or vice versa. However, this method has never been applied in practice. Therefore, this study aims to examine the H&V shield control method, using the developed kinematic shield model for the H&V shield. As a result, the following were found: 1) the calculated shield behavior has an overall good agreement with the planned one; 2) the ground displacement is a predominant factor affecting shield behavior; and 3) the proposed model can simulate the H&V shield behavior reasonably.

KEYWORDS: H&V shield, Articulation angle, Copy cutter range and length, Kinematic shield model.

1. INTRODUCTION

Due to the limited underground space in urban areas and for saving construction cost, the multi-circular face shield (MF shield) (STA 2011a) had been innovated to construct a twin tunnel at once. Furthermore, according to the more severe restrictions of underground space use, the horizontal and vertical variation shield method (H&V shield) (Sonoda et al. 1992; STA 2011b) was innovated, so that the cross section of an MF shield tunnel is changed from horizontal multi-circular shape to vertical one or vice versa. The H&V shield is developed by connecting two articulated shields (Maidl et al. 2012) at their rear bodies and is steered by articulation mechanism and copy cutter, which can be operated individually at each body. These steering options can generate rotating force around the shield axis, which can realize the construction of a spiral tunnel. The example of the H&V shield is shown in Figure 1.



Figure 1 H&V shield. (STA 2011b)

The characteristics of the H&V shield method, compared with other types of shields, are as follows: 1) Tunnel shape and alignment: The H&V shield can construct a separate tunnel and a spiral tunnel, as shown in Figure 2. In the case of a separate tunnel, the H&V shield forms a tunnel with a multi-circular cross section at first, and two ordinary tunnels with a circular cross section after a specified point along the tunnel alignment by splitting the H&V shield to two ordinary shields. On the other hand, in the case of a spiral tunnel, the H&V shield constructs a tunnel with a multi-circular cross section, which is continuously changed from horizontal multi-circular shape to vertical one, or vice versa; 2) Construction period: The H&V shield can shorten a construction period because it can omit an intermediate

vertical shaft to separate the body in the case of a separate tunnel, and can construct multiple tunnels at once in the case of a spiral tunnel; and 3) Construction cost: The H&V shield can save a construction cost because its body can separate without an intermediate vertical shaft and a ground improving work in the case of a separate tunnel, and can reduce the adjacent distance between two circular tunnels in the case of a spiral tunnel.

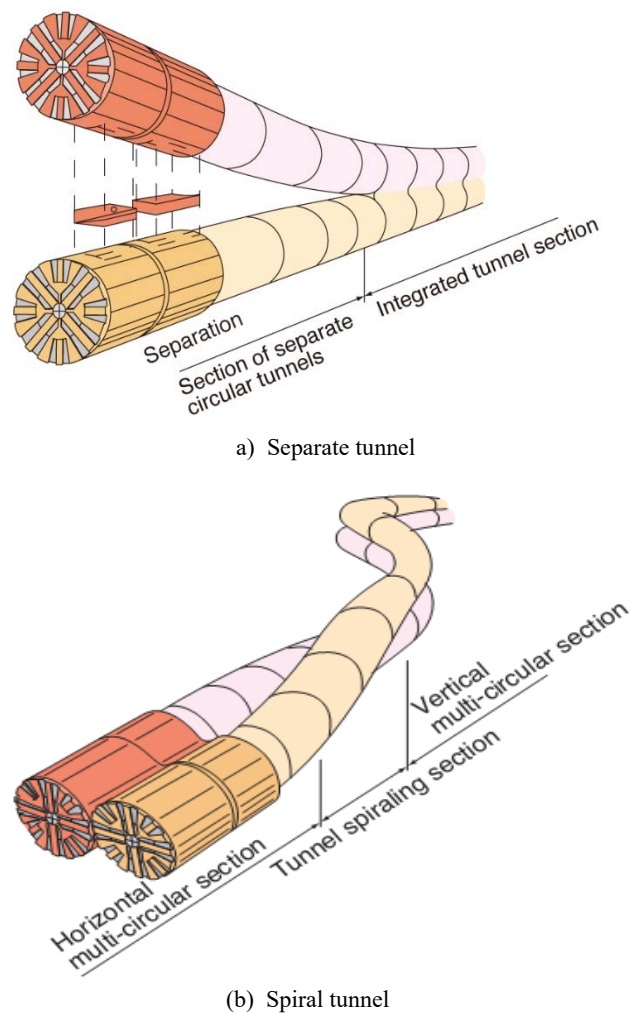


Figure 2 Utilization of H&V shield. (STA 2011b)

Shield is operated for excavation, steering shield, filling up in the tail void, and segment installation mainly. As for steering shield, the shield is controlled by jack, copy cutter and articulation mechanism in practice. The jack generates thrust and horizontal and vertical moments, which can be determined by jack pattern and shield jack pressure. The copy cutter can carry out overcutting with a specified depth and a specified range along the circumference of cutter face. The overcutting by copy cutter defines excavation area and reduces ground reaction force at the overcutting range, which makes the shield rotate toward the overcutting range easily. The articulation mechanism of articulated shield can crease shield with a specified direction and a specified angle. The crease of the shield can reduce ground reaction force at curves by fitting the shield for its excavation area, which makes the shield rotate easily.

The H&V shield for a spiral tunnel can be controlled by spiral jacks, copy cutter and articulation system. The shield jack system including spiral jacks, as shown in Figure 3, causes the eccentric forces to generate torque to twist an H&V shield around its axis. The copy cutter can reduce the ground reaction force at a specified area by overcutting the ground, and the articulation system can also reduce the ground reaction force by articulating the front body from the rear body of each shield, as shown in Figure 4. Using these functions, the H&V shield can rotate around its axis and can advance. Thus, the H&V shield can construct a spiral tunnel.

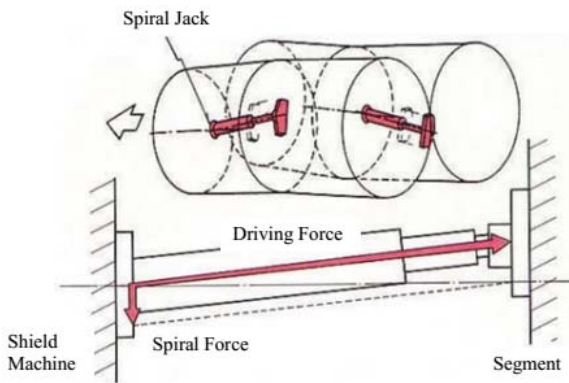


Figure 3 Spiral jack. (STA 2011b)

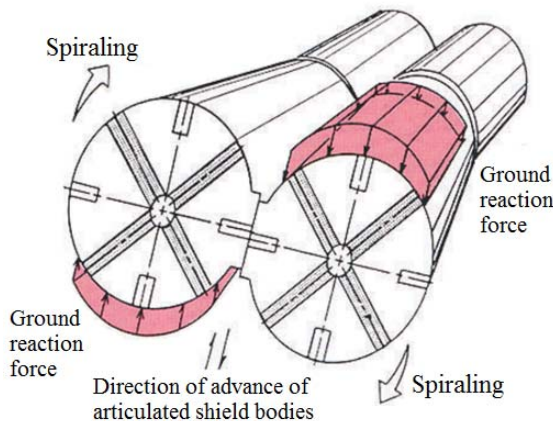


Figure 4 Copy cutter and articulated mechanism in excavation. (STA 2011b)

Recently, the construction project on “Tachiaigawa rainwater discharge tube” has been planned using the H&V shield method to discharge all rainwater in Tachiai river to Keihin channel (Muto et al. 2015). Because of the limitation of land use, such as narrow river and existing structures over the planned route of the tunnel, only the spiral excavation mode of this method can construct the tunnel with a required capacity. However, this is the first application in practice without a test execution. Therefore, this study aims to examine the

H&V shield control method before the construction.

At first, the shield steering parameters, such as copy cutter operation (length and range) and articulation operation (direction and angle), were determined, based on the geometric conditions for both bodies of the H&V shield independently (Chen 2008; Huynh et al. 2015). Thereafter, the jack operation (jack thrust force, horizontal moment and vertical moment) was determined, using the kinematic shield model for the H&V shield, as described below. Next, the H&V shield behavior was simulated using the kinematic shield model for the H&V shield, which has been developed from the one for the single circular shield (Sugimoto et al. 2002; Sramon et al. 2002; Sugimoto et al. 2007), to simulate the H&V shield behavior during excavation theoretically based on equilibrium conditions. In the simulation process, the ground displacement around the shield was taken into account, and the shield operational parameters obtained from the above were also used. In this process, to validate the model performance, the calculated shield behavior was examined from the viewpoint of theory, and the H&V shield control method was confirmed by comparing the calculated shield behavior with the plan data. The force acting at the connection point between the left body and the right body was also calculated for shield design. This paper describes the H&V shield behavior at the sharp curve.

2. METHODOLOGY

The kinematic shield model for single circular shield had been developed, taking into account shield tunnel engineering practices, namely, the excavated area, the tail clearance, the rotation direction of the cutter disc, sliding of the shield, ground loosening at the shield crown, and the dynamic equilibrium condition (Sugimoto et al. 2002). Applying this model to the front and rear sections of both bodies of the H&V shield individually, the H&V model has been developed (Chaiyaput et al. 2015).

The model is composed of five forces: force due to self-weight of machine f_1 , force on shield tail f_2 , force due to jack thrust f_3 , force on cutter disc f_4 , and force on shield periphery f_5 , as shown in Figure 5. The force due to self-weight of machine f_1 and the force on shield periphery f_5 act on the both sections of two bodies. The force on shield tail f_2 acts only on the rear section, whereas the force at face f_4 is loaded on cutter disc of the front section. The force on jack thrust f_3 is composed of the forces due to shield jack and articulated jack. The force on shield periphery f_5 is due to the ground reaction force acting on shield skin plate and the dynamic friction force on shield skin plate.

The interaction force between the shield and the ground can be obtained by considering the coefficient of earth pressure K , which is a function of the distance between the original excavated surface and the shield skin plate U_n shown in Figure 6, where the subscripts h and v are horizontal and vertical directions respectively; the subscripts min , o and max define minimum, initial and maximum respectively; and σ_{vo} is the overburden pressure. In Figure 6, K at $U_n = 0$ means the coefficient of earth pressure at rest, and the gradient of K at $U_n = 0$ represents the coefficient of subgrade reaction k . Furthermore, in the case of soft soil, the ground displacement to shield skin plate can be represented by U_n . On the other hand, for stiff soil, the self-stabilization of the ground can be expected, which causes the appearance of the gap between the shield skin plate and the excavated surface. This consideration is similar to the touching problem in finite element analysis.

The H&V shield behavior is represented by the movement of the shield at the connection point between the left and right body P_c , as shown in Figure 7. The shield behavior during excavation can be obtained by solving the following equilibrium conditions of forces and moments acting on the shield.

$$\begin{bmatrix} \sum_{i=1}^5 (F_{LFi}^M + F_{LRi}^M + F_{RLi}^M + F_{RRi}^M) \\ \sum_{i=1}^5 (M_{LFi}^M + M_{LRi}^M + M_{RLi}^M + M_{RRi}^M) \end{bmatrix} = 0 \quad (1)$$

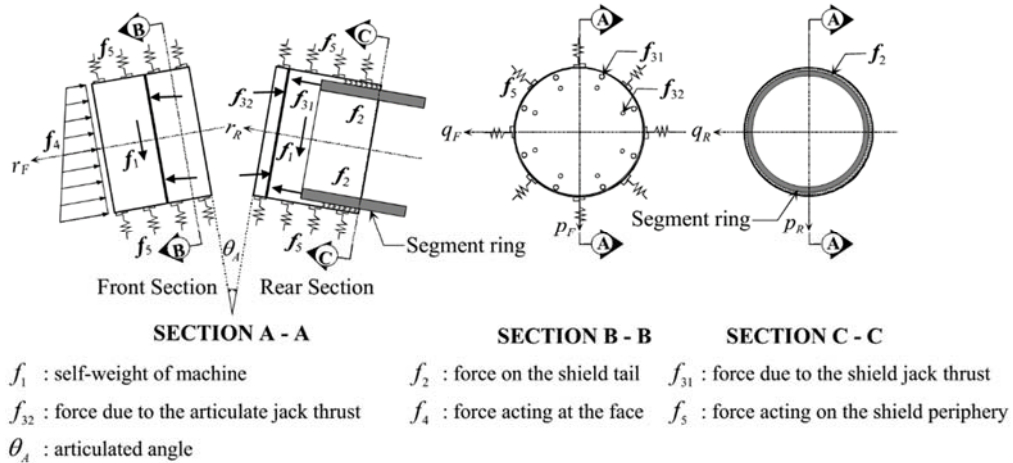


Figure 5 Model of load acting on both front body and rear body

where F and M are the force and moment vectors respectively, the first subscripts L and R denote the left and right bodies of the H&V shield respectively, the second subscripts F and R denote the front and rear sections of each body respectively, and the superscript M indicates the machine coordinate system. It is noted that the force due to articulated jack f_{32} is not necessary to calculate, since the summation of the force due to f_{32} is always zero.

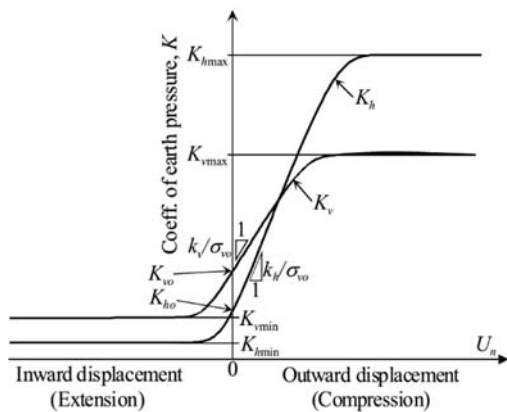


Figure 6 Ground reaction curve

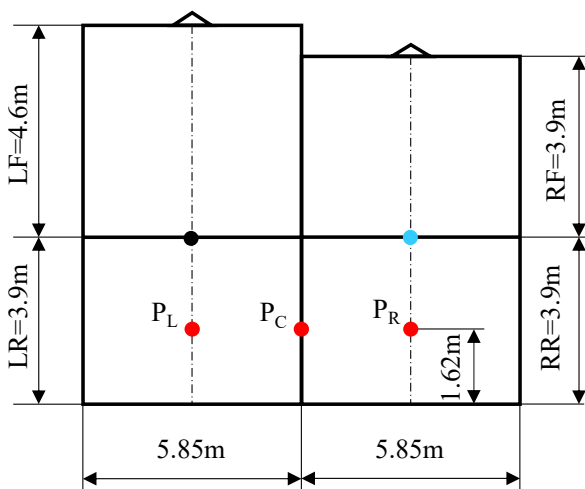


Figure 7 Dimension of the H&V shield machine

3. SITE DESCRIPTION

The target tunnel is Tachiaigawa rainwater discharge tube, where two tunnels are constructed at the same time by the H&V shield. The first one built by the left body of the H&V shield (Tunnel A) is in a horizontal alignment including a leftward curve and a straight line. The second one created by the right body of the H&V shield (Tunnel B) is parallel with Tunnel A in a horizontal plane before rotation around Tunnel A from the rightward transverse direction to the upward vertical one. The plane and longitudinal view of the tunnel and spiral steps are shown in Figure 8. In this study, the segmental ring Nos. 1 to 71 at the sharp curve were used for the analysis, that is, the analysis length is about 40 m. The overburden depth around the analysis area is about 24 m, and the groundwater level is TP-0.97 m. The ground properties are shown in Table 1. The ground reaction curves, $K-U_n$ relationships, used in the kinematic shield model, for Toc, Tos, Tog and Eds layers are shown in Figure 9. The dimensions of the tunnel and the shield are shown in Table 2 and Figure 7 where LF, LR, RF and RR are the left front, left rear, right front and right rear bodies respectively. Tunnels A and B are constructed in layers Toc, Tog, Tos and Eds, as shown in the longitudinal tunnel view of Figure 8, by the H&V shield with 2.925 m in outer radius of both shields and 8.5 m for the left and 7.8 m for the right body in total length.

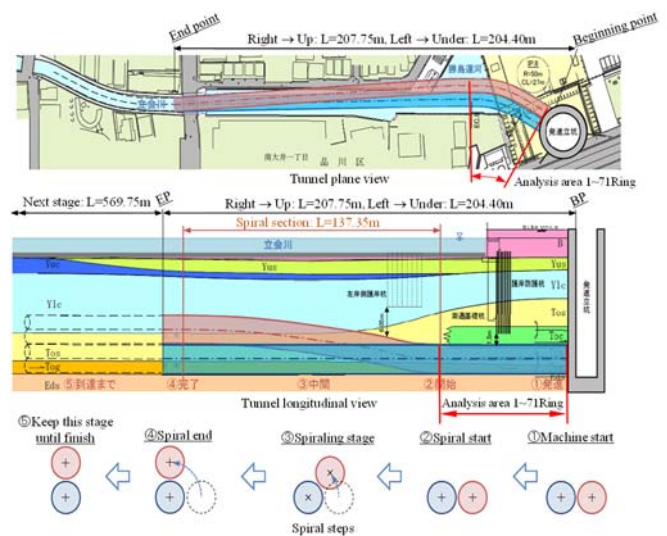


Figure 8 Site location and geological profile

Table 1 Ground properties

Ground layer	Toc	Tos	Tog	Eds
Unit weight (kN/m ³)	17	19	20	19
Cohesion (kN/m ²)	98	9.8	0	0
Internal friction angle (deg)	0	35	40	35
K_{ha} ($\sim K_{hmin}$)	0	0	0	0
K_{ho}	1	0.426	0.357	0.426
K_{hp} ($\sim K_{hmax}$)	5	5	5	5
K_{va} ($\sim K_{vmin}$)	0	0	0	0
K_{vo}	1	1	1	1
K_{vp} ($\sim K_{vmax}$)	5	5	5	5
k_h (MN/m ³)	13.6	37.1	49.3	47.3
k_v (MN/m ³)	13.6	37.1	49.3	47.3
Coeff. of friction	0.1	0.1	0.1	0.1

Table 2 Dimensions of tunnel and shield

Item	Component	Left body	Right body
Shield	Outer radius (m)	2.925	2.925
	Total length (m)	8.5	7.8
	Length of front body (m)	4.6	3.9
	Length of rear body (m)	3.9	3.9
	Self-weight (kN)	2830	2750
Shield jack	Number of jacks	20	20
	Radius of jack (m)	2.6	2.6
Articulated jack	Number of jacks	12	12
	Radius of jack (m)	2.025	2.025
Segment	Outer radius (m)	2.8; 2.85	2.8; 2.85
	Width (m)	0.501; 1.2	0.561; 1.2
Tunnel	Horizontal curve radius (m)	50.00	55.94
Ground	Ground water level (m)	TP-0.97	
	Overburden depth (m)	24	

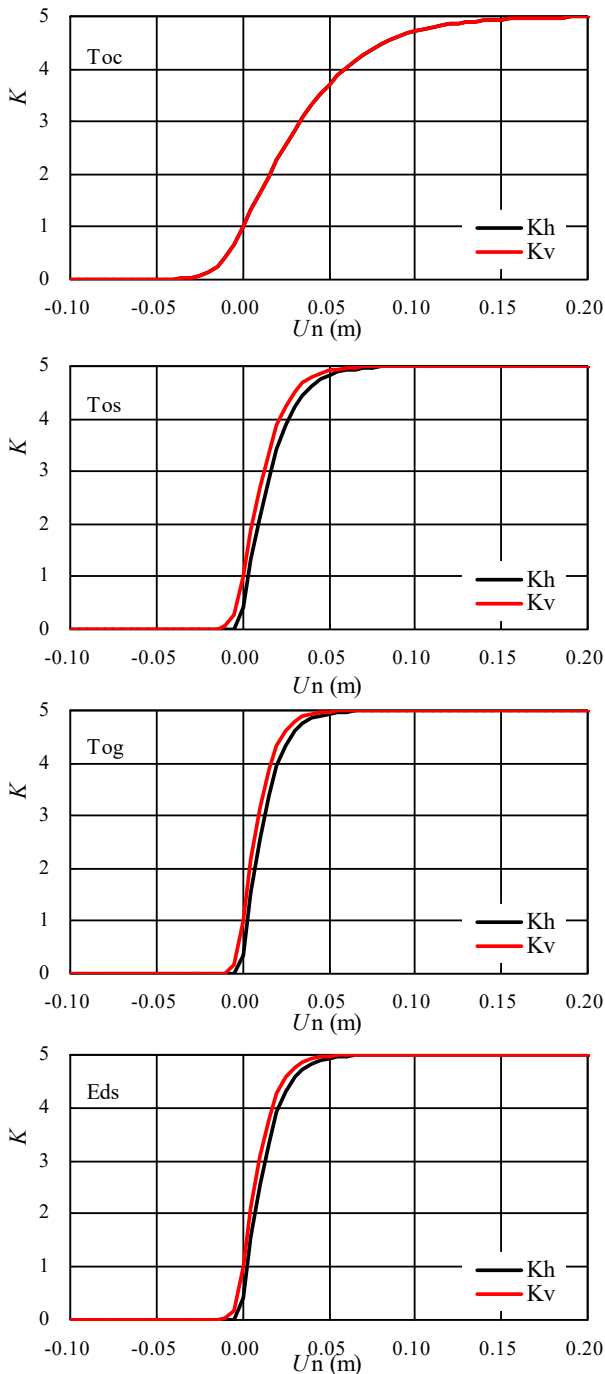


Figure 9 Ground reaction curve of the soils at the tunnel

4. SIMULATION OF H&V SHIELD EXCAVATION

4.1. Operation data

The input data used for simulation are shown in Figure 10. The tunneling operations are jack thrust F_{3r} , horizontal jack moment M_{3p} (+: right turn), vertical jack moment M_{3q} (+: downward), cutter face rotation direction CF (1: counterclockwise direction, viewed from shield tail), copy cutter length CCL , area of applied copy cutter CC range, and articulation angle in horizontal direction θ_H (+: left turn), which are employed to control the shield position and the shield behavior during excavation. The behavior of both shields is defined as yawing angle ϕ_y (+: right turn), pitching angle ϕ_p (+: downward), and rolling angle ϕ_r (+: clockwise direction, viewed from shield tail). The excavation conditions are shield velocity v_s , slurry pressure σ_m and slurry density γ_m in the chamber, which is usually controlled to stabilize the tunnel face.

F_{3r} of about 10 MN is applied to the shield to drive the shield forward against earth pressure at the face and friction on the shield skin plate as its advance. Since both tunnel planned alignments at the analysis area are horizontal leftward curves, M_{3p} is applied to negotiate the horizontal moment due to normal earth pressure around skin plate M_{5p} , which gets much influence of no earth pressure around the connection point of the rear body. M_{3q} is mainly applied against the vertical moment due to the earth pressure on the cutter disc and the self-weight of the shield. The value of the abovementioned three parameters is determined through two steps. First, the forces and moments generated on the H&V shield are calculated without the jack force (F_{3r} , M_{3p} and M_{3q} are zero). The used simulation model will be presented in the next section. From the results of this step, the initial values of the jack force are defined. Second, those values will be modified aiming to keep the H&V shield following the planned tunnel alignment. The most optimal values will be obtained when the agreement between the calculated and planned data has been achieved.

CF defines the rotation direction of cutter torque, which is generated due to the shearing resistance on the cutter disc, and its rotation direction causes the shield rolling around its axis. Therefore, the rotation direction of the cutter disc is alternately controlled to maintain the use of facilities inside the shield. Since the tunnel is excavated at the curved alignment, the copy cutter is employed at around the left spring line of the shield for the leftward curve. The copy cutter is used to increase the excavated area around the cutter disc, which reduces the ground reaction force acting on the skin plate and makes a shield easily translate or rotate to this field. θ_H of the left and right bodies at the leftward curve are about 270 min and 240 min respectively, which correspond to the radius of curvature of the horizontal alignment of both tunnels. It means that the horizontal curve radius of Tunnel A is less than that of Tunnel B. The use of articulation of shield is to fit the skin plate to the excavated area by cutter disk and copy cutter, which also reduces the ground reaction

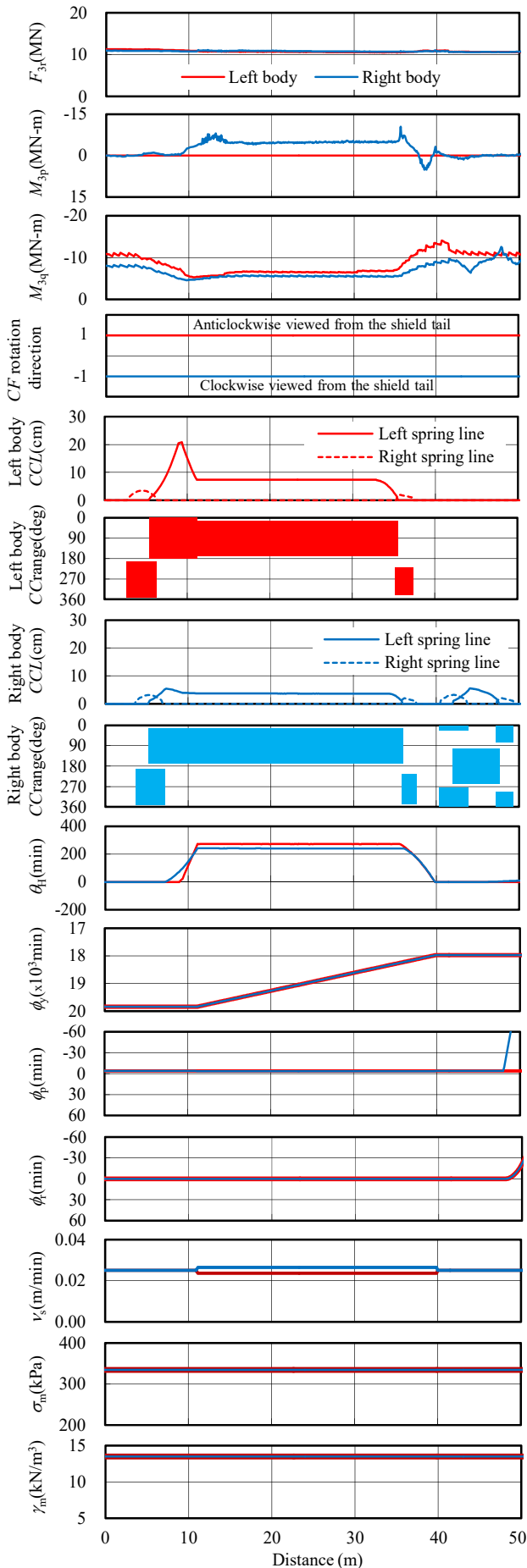


Figure 10 Shield tunneling input data

force acting on the surface plate and makes a shield easily translate or rotate.

ϕ_y shows that both bodies' rotation follows the planned horizontal tunnel alignment at the leftward curve. ϕ_b and ϕ_r are zero because the H&V shield is on a horizontal plane and its components (the left and right bodies) do not rotate around their axis.

Shield velocity v_s of 0.025 m/min and γ_m of 13.5 kN/m³ were set, based on the experience. To stabilize the face, σ_m about 334 kPa is applied based on the lateral earth pressure at the tunnel face.

4.2 Simulation results

The shield behavior is then simulated from Ring Nos. 1 to 71, using the operational control data and the excavation condition in Figure 10.

4.2.1 H&V shield behavior

Figure 11 shows the planned alignment and the calculated traces of the left and right bodies of the H&V shield on vertical and horizontal planes. The calculated and planned time-dependent parameters ϕ_y , ϕ_p , ϕ_r and v_s are compared in Figure 12. Figure 11 shows that the maximum difference between the planned alignment and the calculated traces is 1.8 cm and 2.7 cm for the vertical position of the left and right bodies respectively and is 32.5 cm for the horizontal position of both bodies. In Figure 12, the calculated ϕ_y indicates that the shield performs good negotiation to the sharp leftward curve. The calculated ϕ_p shows the lookup of 30 minutes at the end of the leftward curve (around the distance 40 m), compared with the planned ϕ_p , and the ϕ_p along the longitudinal tunnel alignment up to the distance 33 m is within 15 minutes' lookup. The calculated ϕ_r at the sharp curve gradually decreases from the start to the end of the curve up to 24 minutes, that is, the H&V shield rotates to counterclockwise viewed from tail. The calculated v_s , with the maximum difference from the planned v_s just 0.6 mm/min, nearly coincides with the planned one. Therefore, these figures, in general, show overall good agreement between the calculations and the plan of shield behavior. Considering the change of geological conditions along the longitudinal tunnel alignment and the connection condition between the right and left rear bodies of the H&V shield, these differences can be adjustable by updating the shield operation on time, based on real-time measurement on shield position, rotation, etc.

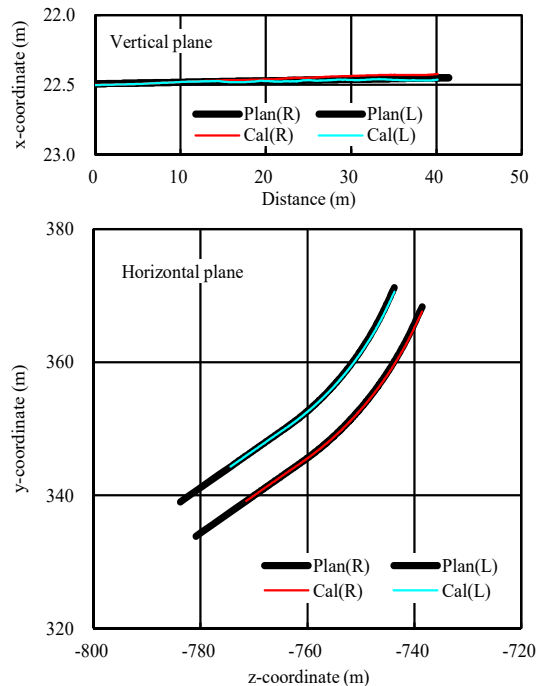


Figure 11 Calculated and planned shield traces

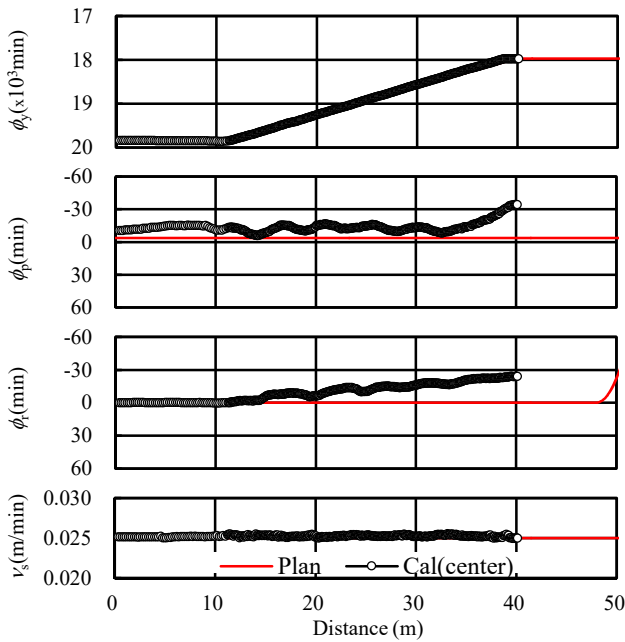


Figure 12 Calculated and planned shield behavior

4.2.2 Ground-shield interaction

The forces and moments described hereafter are considered at the distance of 4.345 m on the straight line and 22.574 m on the sharp curve as an example. The distance between the original excavated surface and the shield skin plate U_n around the shield skin plate are shown in Figures 13 and 14 and the effective normal earth pressure acting on the shield periphery σ_n' is plotted in Figures 15 and 16, where the shield skin plate is unfolded as a flat plate, that is, the vertical axis shows the length of the shield and the horizontal axis represents the circumference of the shield. σ_n' is determined by applying U_n to the ground reaction curve in Figure 9.

In case of excavation at the straight line, the following are found from Figure 13: 1) U_n at almost all of the area is a negative value. This is because of the overcutting by cutter face and copy cutter; 2) U_n becomes positive in a little area at the invert around the tail of both bodies, where the H&V shield skin plate pushes the ground. At the opposite side (the crown around the tail of both bodies), U_n becomes negative, where the earth pressure is in active state. These characteristics result from the equilibrium condition; 3) The contour line becomes intense at the right spring line (from 180 to 360 degree) around the cutter face of both bodies. This comes from the application of copy cutter shown in the copy cutter range of Figure 10; and 4) The distribution of U_n at the both right and left bodies is almost same. This phenomenon is natural when the shield is in the straight line and prepares to enter the leftward curve. From Figure 15, the following are found: 1) σ_n' is close to zero in the almost area because of the self-stabilization of the ground due to the gap between the excavated surface and the shield skin plate; 2) The high intensity of σ_n' appears in the area where U_n is positive, which is reasonable from the viewpoint of ground-structure interaction; 3) σ_n' is zero at the area where the copy cutter is applied. This means that the shield does not touch the ground; and 4) σ_n' around both spring lines of both bodies is smaller than that at the invert and crown of both bodies. This is because the horizontal effective earth pressure is smaller than the vertical one due to smaller K_{ho} than K_{vo} , as shown in Table 1.

When the H&V shield excavates at the sharp curve, the following are found from Figure 14: 1) U_n at the almost area is negative. This corresponds to the overcutting by cutter face and copy cutter; 2) U_n becomes positive along the invert of the rear left body and around the end of the right spring line of the rear right body. The H&V shield pushes the ground at these locations, whereas U_n at the opposite side becomes negative. These characteristics result from the equilibrium

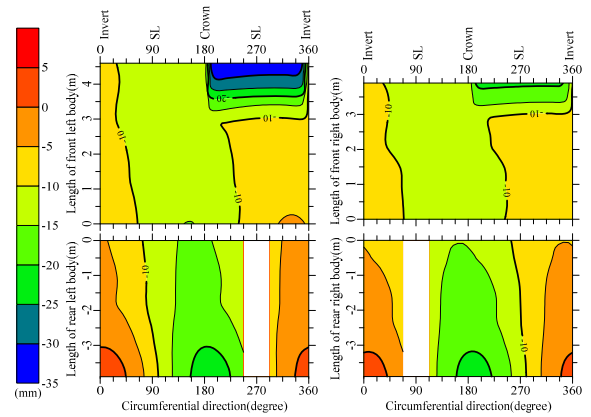


Figure 13 U_n around shield on the straight line at 4.345 m

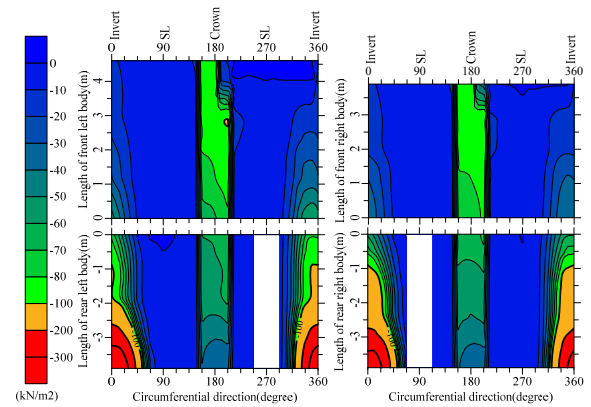


Figure 14 σ_n' around shield on the straight line at 4.345m

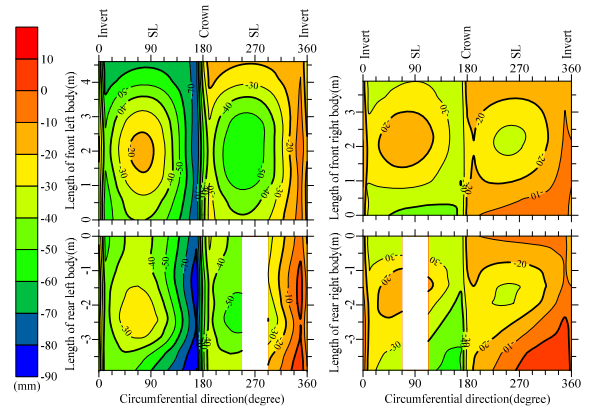


Figure 15 U_n around shield on the sharp curve at 22.574m

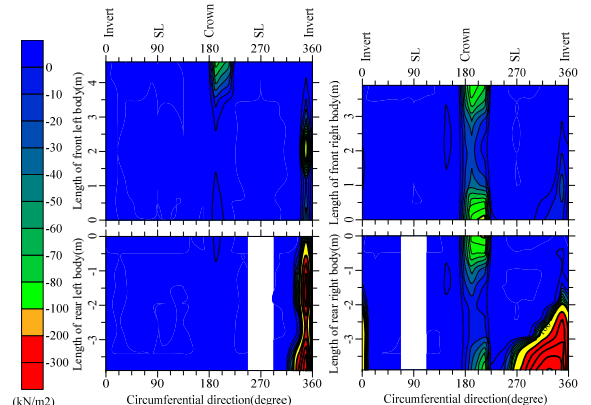


Figure 16 σ_n' around shield on the sharp curve at 22.574m

condition and correspond to the leftward curve of the tunnel alignment; 3) The contour line at the crown and the invert of both bodies becomes intense. This is because of the application of copy cutter shown on the copy cutter range of Figure 10; and 4) U_n along the left spring line at the middle position of each body is larger than that at the end position of each body, while U_n along the right spring line has a reverse tendency. These come from the geometric condition between the shield and the excavated area. From Figure 16, the following are found: 1) the intensity of σ_n also appears in the area where U_n is positive due to ground-structure interaction; and 2) σ_n is close to zero in the almost area. This can be explained as the same reasons in Figure 15.

4.2.3 Forces and moments acting on the shield

The forces and moments acting on the shield at the distance 4.345 m and 22.574 m are summarized in Tables 3 and 4 respectively, where F and M are the force and the moment acting on the shield respectively; the subscripts p, q and r are the directions in the machine coordinate system in Figure 5; and the subscript numbers are the types of the forces in Figure 5. From these tables, the following are found: 1) The forces and moments in these tables indicate that they satisfy the equilibrium conditions; 2) The total amount of each component of forces and moments at the connection point is the interaction one between the left and right bodies. The forces in transverse direction F_q acting at the connection point between the left and right bodies is about 3000 kN, since the connection area has no earth pressure, then each body pushes the opposite side body. The moment around shield axis M_r from the right body to the left body at the connection point is about -3300 kN-m. This means that the right body generates the M_r , so that the left body rotates around the shield axis to a counterclockwise direction. This calculated M_r coincides with the rolling angle ϕ of the left and right bodies in Figure 12. Other components of forces and moments are not so large; and 3) This result indicates that proper shield operation of the left and right bodies is necessary to escape excess forces and moments at the connection point, taking the interaction forces and moments at the connection point into account.

Table 3 Force and moment acting on shield (Distance 4.345 m)

Type Body	Force and moment components (kN, kN-m)						
	F_p	F_q	F_r	M_p	M_q	M_r	
f_1	Front left	1340	0	-5	-16	6271	-3980
	Rear left	1490	0	-6	-18	2131	-4425
	Front right	1260	0	-5	14	5569	3742
	Rear right	1490	0	-6	17	2131	4425
f_2	Front left	0	0	0	0	0	0
	Rear left	0	0	0	0	0	0
	Front right	0	0	0	0	0	0
	Rear right	0	0	0	0	0	0
f_3	Front left	0	0	0	0	0	0
	Rear left	0	0	11211	32791	-9647	0
	Front right	0	0	0	0	0	0
	Rear right	0	0	10893	-32110	-7464	0
f_4	Front left	331	39	-10595	-31737	2090	2435
	Rear left	0	0	0	0	0	0
	Front right	154	-38	-10592	31694	986	-2924
	Rear right	0	0	0	0	0	0
f_5	Front left	-537	57	-159	-549	-2398	1595
	Rear left	-2618	-2568	-302	-266	1027	7774
	Front right	-372	41	-139	311	-1591	-1104
	Rear right	-2538	2469	-293	-132	895	-7539
Σf	Left body	7	-2472	143	205	-526	3399
	Right body	-7	2472	-143	-205	526	-3399
	Whole body	0	0	0	0	0	0

Table 4 Force and moment acting on shield (Distance 22.574m)

Type Body	Force and moment components (kN, kN-m)						
	F_p	F_q	F_r	M_p	M_q	M_r	
f_1	Front left	1340	5	-5	-39	6261	-4234
	Rear left	1490	6	-5	-24	2131	-4425
	Front right	1260	5	-4	-9	5563	3553
	Rear right	1490	6	-5	8	2131	4425
f_2	Front left	0	0	0	0	0	0
	Rear left	0	0	0	0	0	0
	Front right	0	0	0	0	0	0
	Rear right	0	0	0	0	0	0
f_3	Front left	0	0	0	0	0	0
	Rear left	-1	0	10647	31142	-6589	4
	Front right	0	0	0	0	0	0
	Rear right	1	0	10802	-36357	-5689	4
f_4	Front left	349	-794	-10411	-29224	2327	2243
	Rear left	0	0	0	0	0	0
	Front right	167	-772	-10570	33313	666	-2911
	Rear right	0	0	0	0	0	0
f_5	Front left	-1242	63	-33	-408	-5510	3901
	Rear left	-1979	-2270	-107	631	31	5879
	Front right	-688	136	-69	-267	-2965	-1945
	Rear right	-2186	3615	-239	1234	1645	-6494
Σf	Left body	-43	-2990	86	2078	-1349	3368
	Right body	43	2990	-86	-2078	1349	-3368
	Whole body	0	0	0	0	0	0

5. CONCLUSIONS

The simulation of H&V shield behavior at a straight line and curved alignment in a multilayered ground was carried out using the proposed kinematic shield model for the H&V shield and the input data, as shown in Figure 10, to examine the H&V shield control method. The verification was conducted by comparing the calculated shield behavior with the planned one. As a result, the following can be concluded:

1. The calculated H&V shield behavior is reasonable from the viewpoint of theory and site experience.
2. The calculated shield behavior has an overall good agreement with the planned one.
3. The ground displacement, which is defined by the excavated area including the area excavated by copy cutter and the articulation of the H&V shield, is a predominant factor affecting shield behavior since it defines the ground reaction force acting on the shield. These facts also coincide with the practical experience.
4. The proper shield operation of both bodies is important, taking the interaction forces and moments at the connection point into account.
5. The abovementioned examinations indicate that the proposed model for the H&V shield can simulate the H&V shield behavior reasonably.

6. ACKNOWLEDGEMENTS

The authors gratefully acknowledge the Bureau of Sewerage, Tokyo Metropolitan Government in Japan who provided the site data.

7. REFERENCES

Chaiyaput, S., Huynh, T. N., and Sugimoto, M. (2015) "Influence of copy cutter length on H&V shield behavior", 15th Asian Regional Conference on Soil Mechanics and Geotechnical Engineering (15ARC), Fukuoka, Japan, ISSMGE.

Chen, J. (2008) Study on calculation method of overcutting space and articulation angle during curved excavation by articulated shield, PhD thesis, Nagaoka Univ. of Technology, Niigata, Japan.

- Huynh, T. N., Chen, J., and Sugimoto, M. (2015) "Analysis on shield operational parameters to steer articulated shield", 15th Asian Regional Conference on Soil Mechanics and Geotechnical Engineering (15ARC), Fukuoka, Japan, ISSMGE.
- Maidl, B., Herrenknecht, M., Maidl, U., and Wehrmeyer, G. (2012) *Mechanized shield tunnelling*, 2nd edition, Ernst & Sohn, Berlin, Germany.
- Muto, M., Ito, T., Usui, H., and Ishido, A. (2015) "Drive shield TBM longitudinally under a small river using the H&V shield spiral technique", *Tunnel and Underground Space*, Japan Tunnelling Association, 46(2), 17–23 (in Japanese).
- Shield Tunnelling Association in Japan (2011a) *Technical note on multi-circular face shield method*, 6th edition, Japan, STA (in Japanese).
- Shield Tunnelling Association in Japan (2011b) *Technical note on Horizontal & vertical variation shield method*, 6th edition, Japan, STA (in Japanese).
- Sonoda, T., Hagiwara, H., Osaki, H., Noguchi T., and Nakamura, M. (1992) "Construction of underground space by a new shield tunnelling method: Spiral tunnelling and ramification of multi-circular face shield", *Tunnelling and Underground Space Technology*, 7(4), 355–361.
- Sramoon, A., Sugimoto, M., and Kayukawa, K. (2002) "Theoretical model of shield behavior during excavation: II. Application", *J. of Geotechnical and Geoenvironmental Engineering*, ASCE, 128(2), 156–165.
- Sugimoto, M., and Sramoon, A. (2002) "Theoretical model of shield behavior during excavation: I. Theory", *J. of Geotechnical and Geoenvironmental Engineering*, ASCE, 128(2), 138–155.
- Sugimoto, M., Sramoon, A., Konishi, S., and Sato, Y. (2007) "Simulation of shield tunneling behavior along a curved alignment in a multilayered ground", *J. of Geotechnical and Geoenvironmental Engineering*, ASCE, 133(6), 684–694.